Methane oxidation using Au/MgO catalysts

Keith Blick [a], Thanos D. Mitrelias [b], Justin S.J. Hargreaves [c], Graham J. Hutchings [a], Richard W. Joyner [c], Christopher J. Kiely [b] and Fritz E. Wagner [d]

[a] *Leverhulme Centre for Innovative Catalysis, Department of Chemistry, University of Liverpool, Liverpool L69 3BX, UK*
[b] *Department of Materials Science, University of Liverpool, Liverpool L69 3BX, UK*
[c] *Catalysis Research Centre, Nottingham Trent University, Clifton Lane, Nottingham NG11 8NS, UK*
[d] *Physics Department, Technical University of Munich, D-8046 Garching, Germany*

Received 12 July 1997; accepted 18 December 1997

A series of Au/MgO (0.04–15 wt%) catalysts have been investigated for the oxidation of methane. Detailed electron microscopy and Mössbauer spectroscopy studies show that two distinct Au morphologies can be observed: (a) two-dimensional Au rafts and (b) discrete three-dimensional Au particles (5–10 nm in diameter). The two-dimensional rafts are observed as the main form of Au at low loadings and, interestingly, these are observed to poison the methane coupling activity of MgO. As the Au loading is increased the proportion of Au present as discrete particles increases and these are considered to be active for methane oxidation to CO and CO_2.

Keywords: methane oxidation, gold, magnesium oxide

1. Introduction

Gold is not often considered as a metal of choice for a particular catalytic reaction and, compared with other precious metals, it has found very limited application in heterogeneous catalysis. There have been, however, two recent examples for which supported gold catalysts are indeed the best heterogeneous catalysts, namely the hydrochlorination of acetylene to form vinyl chloride [1–3] and the oxidation of carbon monoxide at ambient temperature [4–6]. In the former example the best activity is observed with 2 wt% Au supported on activated carbon. The catalytic activity in this case is related to the concentration of Au(I) and the deactivation of these catalysts is related to the formation of metallic gold [2]. In contrast, small Au particles (ca. 5 nm in diameter) are considered to be the active form of gold for the oxidation of carbon monoxide. In this case the nature of the support is found to be important [4]. In particular, Au/MgO has been found to be an especially active catalyst and Haruta et al. have indicated that this catalyst can be effective for the reaction at sub-ambient temperatures as low as 198 K. More recently [7], Haruta et al. have shown that supported gold catalysts are also effective for the total oxidation of propene at elevated temperatures and in this case Au/TiO_2 demonstrates high activity. In both of these catalytic applications the optimum gold loading appears to be in the range 2–5 wt% and in general there are few investigations reported involving gold concentrations that are much higher or lower than this preferred range.

In this paper we consider the use of Au/MgO as a catalyst for the oxidation of methane. Methane oxidation has been extensively studied with MgO based catalysts [8–12]. Although MgO alone can be an active catalyst, significant enhancement in the catalytic activity is observed when the MgO is doped with appropriate cations. For example, Li-doping causes an increase in both methane conversion and C_2 hydrocarbon selectivity, and this enhancement has been correlated with the formation of line defects of the type $a/2\langle 110\rangle$ [11]. In this study we use a combination of characterisation techniques, including transmission electron microscopy and Mössbauer spectroscopy, to characterise a series of Au/MgO catalysts and correlate these structural data with the catalytic performance.

2. Experimental

Catalyst preparation. Magnesium hydroxide (Merck, ultrapure) was pelleted and sieved to a particle size of 600–1000 μm and calcined in air (450°C, 24 h; 800°C, 24 h) to produce MgO. The MgO was then impregnated with an aqueous solution of chloroauric acid, and multiple impregnations were used to obtain the desired Au loadings. The material was dried (110°C, 16 h), calcined (800°C, 3 h), and then cooled and stored in a desiccator prior to use as a catalyst. The undoped MgO was prepared in an analogous manner.

Catalyst testing. The catalysts were tested for the oxidation of methane in a fixed bed laboratory microreactor constructed from quartz glass [11]. The reactants methane (46%, BOC, 99.0%) and oxygen (8%, BOC, 99.6%) were diluted with helium (46%, BOC, 99.995%) and passed over the catalyst (2 g, 750°C, atmospheric

pressure) at a gas hourly space velocity of 750 h^{-1}. The products were analysed using on-line gas chromatography.

Catalyst characterisation. The elemental composition was determined using inductively coupled plasma optical emission spectroscopy (ARL 3520 spectrometer) and surface areas were determined according to the BET method (Micromeritics ASAP 2400). The Mössbauer spectra were measured at 4.2 K with the 77 keV resonance of ^{197}Au. Sources of ^{197}Pt ($t_{1/2} = 18$ h) in isotopically enriched ^{196}Pt metal were used. The spectra were fitted with appropriate superpositions of Lorentzian lines. Electron microscopy studies were carried out in a JEOL 2000EX transmission electron microscope operating at 200 kV. TEM samples were prepared by dispersing the catalyst powder onto a lacey carbon film supported on a copper mesh grid.

3. Results

3.1. Oxidation of methane using Au/MgO catalysts

Au/MgO catalysts were prepared with a range of Au loadings and these were investigated for the oxidation of methane at 750°C. The results are given in table 1 together with those for undoped MgO tested under the same conditions. For MgO at this temperature the main carbon containing products were C_2 hydrocarbons and carbon oxides. These products are consistent with those observed in previous studies [11,12], and the C_2 hydrocarbons and CO originate from the oxidative coupling of methane, a gas phase radical reaction initiated by the MgO surface [11]. Addition of 0.04 wt% Au has a dramatic effect on the catalyst activity. The intrinsic methane conversion activity decreases markedly although the surface area increases. The decrease in conversion is due, almost exclusively, to a decrease in the formation of the products of the oxidative coupling reaction, i.e. C_2 hydrocarbons and CO. Higher Au loadings lead to a general decrease in surface area and an increase in the intrinsic activity. As the Au loading increases further, the hydrocarbon yield decreases and the yields of CO and CO_2 increase.

3.2. Mössbauer spectroscopy studies

^{197}Au Mössbauer spectroscopy is well suited to identify the chemical state of gold on supported Au catalysts [2]. Samples containing 0.04, 1, 5, 15 wt% Au were studied at 4.2 K; the Mössbauer spectra are shown in figure 1. Samples containing 1, 5 and 15% Au all exhibit a single narrow line with an isomer shift of -1.24 mm s^{-1} which can be assigned to metallic Au (isomer shift of pure Au metal is 1.23 mm s^{-1}). The linewidths for these samples (table 2) are slightly broader than that observed in a thin absorber of bulk Au (1.89 mm s^{-1}), but this is considered to be due to the broadening arising from the finite absorber thickness.

The ^{197}Au Mössbauer spectrum for the 0.04 wt% Au/MgO sample shows an additional feature. In addition to the line assigned to metallic Au at -1.24 mm s^{-1}, there is an additional line at 1.38 mm s^{-1} which accounts for ca. 15% of the spectral intensity. The line for metallic Au is somewhat broadened when compared with the other samples (2.27 mm s^{-1}) which in this case is considered to be due to the nature of the thin Au films present in the sample. In general with metal particles, as the particle size decreases the isomer shift for the metal line becomes more positive. This effect is, however, small (ca. 0.1 mm s^{-1}) and the effect has not been observed with Au on any support to date. The line at 1.38 mm s^{-1} is, therefore, not considered to be due to a particle size effect. The effect is consistent either with diffusion of the Au into the MgO support or the formation of Au thin films since in both cases this would increase the interaction between the Au and the lattice O^{2-} of MgO and this would result in a positive isomer shift.

3.3. Electron microscopy studies

A representative bright-field electron micrograph of

Table 1
Methane oxidation using Au/MgO catalysts [a]

Au (wt%)	Surface area (m^2 g^{-1})	Conversion (%)		Product yield [b] (%)				Intrinsic activity [c] (10^4 mol h^{-1} g^{-1})
		CH_4	O_2	C_2H_6	C_2H_4	CO_2	CO	
0	23	14.3	99.8	0.74	0.91	3.78	1.78	1.85
0.04	30	10.7	99.8	0.52	0.22	3.50	0.82	1.03
0.1	25	9.2	99.3	0.27	0.13	3.38	1.26	1.06
1.0	17	8.7	88.4	0.11	0.06	2.68	1.44	1.46
2.0	14	9.0	87.1	0.08	0.02	2.81	1.50	1.90
3.0	12	9.3	86.2	0.14	0.09	3.18	1.20	2.29
5.0	9	9.8	99.8	0.06	trace	3.31	1.18	3.22
10.0	6	9.2	99.4	0.11	0.1	3.88	0.47	3.80

[a] 750°C, $CH_4/O_2/He = 46/8/46$.
[b] Yield = methane conversion × product selectivity.
[c] Intrinsic activity for methane conversion.

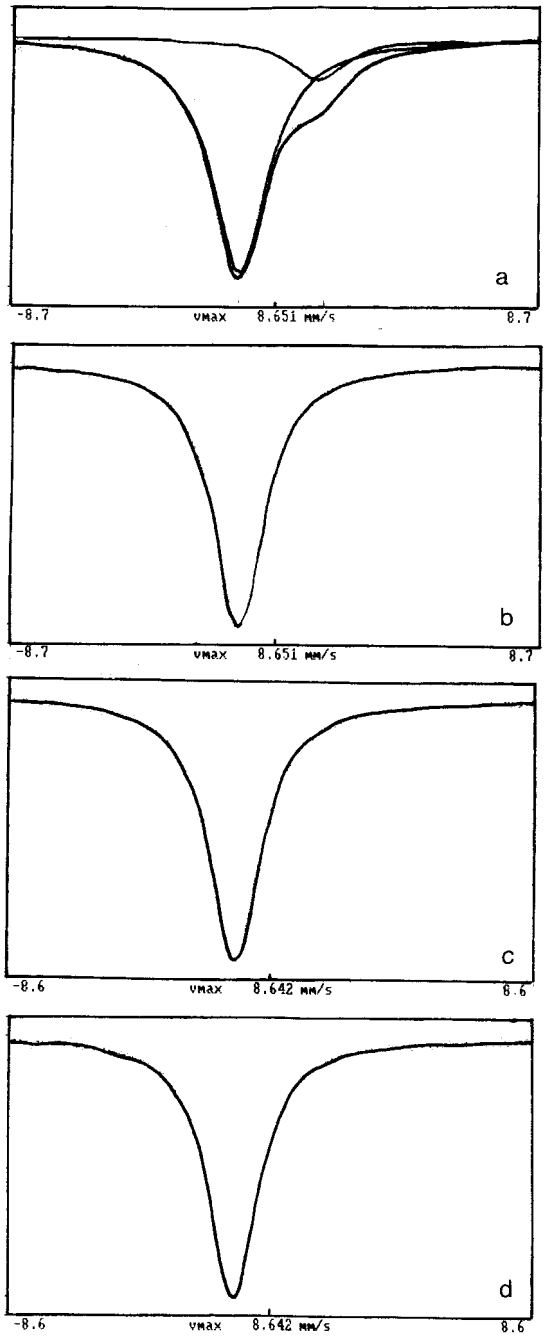

Figure 1. ^{197}Au Mössbauer spectra for various Au/MgO samples, (a) 0.04 wt% Au, (b) 1 wt% Au, (c) 5 wt% Au, (d) 15 wt% Au.

the undoped MgO is shown in figure 2a. The material has a blocky morphology that is very characteristic of the ex-hydroxide material [11]. Figures 2b–2e show comparable micrographs for samples doped with 0.11, 1.5, 4.1 and 15 wt% Au respectively. The average sizes of the MgO grains increase systematically from 40 nm in the undoped material up to 1000 nm in the 15 wt% Au/MgO sample, even though the calcination treatment that each specimen received was identical.

Figure 3a shows an HREM micrograph of the pure MgO in which it is clear that the surface structure is

Table 2
Calculated Mössbauer parameters for Au/MgO catalysts at 4.2 K

Au (wt%)	Line 1 (mm s^{-1})		Line 2 (mm s^{-1}) isomer shift
	isomer shift	linewidth	
0.04	−1.24110	2.26844	1.38042
1.0	−1.23819	2.01208	–
5.0	−1.24366	2.10197	–
15.0	−1.24344	2.01589	–

made up of a multitude of {100} crystal planes. A corresponding high density of step edges and corner sites arise as a consequence of the numerous {100} crystal plane intersections. When this is compared to any of the samples loaded with Au (figure 3b) the same facet structure is apparent. However, there are additional distinct patches of moiré fringes present which can be as large as 20 nm in size. Such interference fringes occur when two crystalline materials overlap along the incident beam direction, and are most likely caused by the presence of thin rafts of crystalline Au on the MgO support. These patches are highly mobile under the influence of the electron beam and tend to disappear within a few seconds. This suggests that under electron bombardment the Au is being atomically dispersed either by spreading over the surface or by migration into the MgO support. Previous studies by Ajayan and Marks [13,14] have shown that small Au particles can diffuse into MgO when exposed to low electron beam doses.

Discrete Au particles were only observed in samples containing more than 1.5 wt% Au. Such particles were usually spherical in shape, although close inspection shows them to be composed of {111} and {100} cube-octahedral crystal planes as shown in figure 4. In general, the Au particles were in the size range 5–10 nm, although occasional particles up to 50 nm in diameter were found in the 15 wt% Au sample. Although the average Au particle size was similar for all the samples in the 1.5–15 wt% doping range, the number density of particles increased with increasing Au content.

4. Discussion

4.1. Structure of Au/MgO catalysts

The addition of Au to MgO using an impregnation method has a significant effect on the structure, depending on the doping level of Au used. One of the most noticeable effects is that the crystallite size of MgO progressively increases as the Au concentration is increased. Since Au seems to promote sintering and grain growth in MgO, one might expect that it does so by enhancing the point defect population and hence the bulk diffusion kinetics. It is, however, very unlikely that Au^+ (1.37 Å)

a

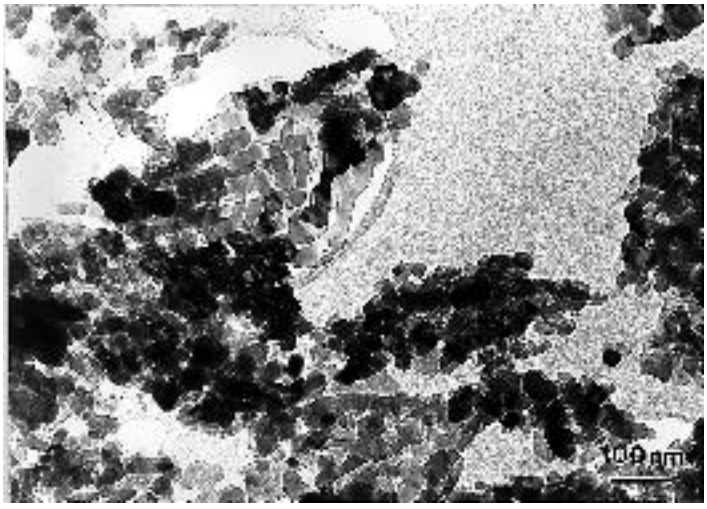

b

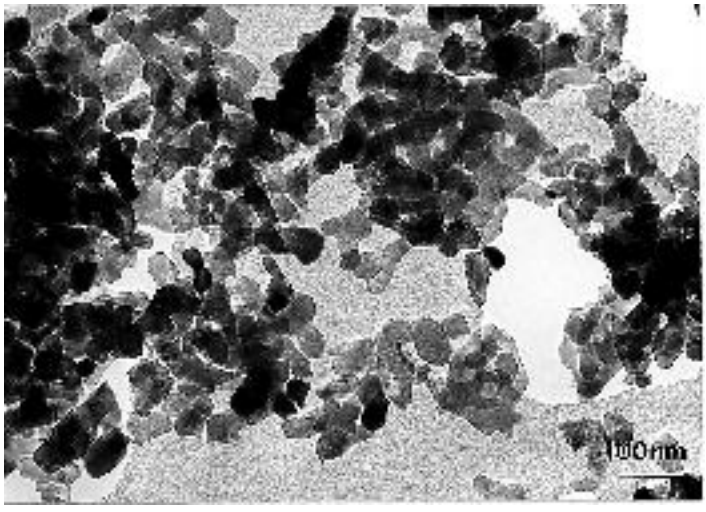

c

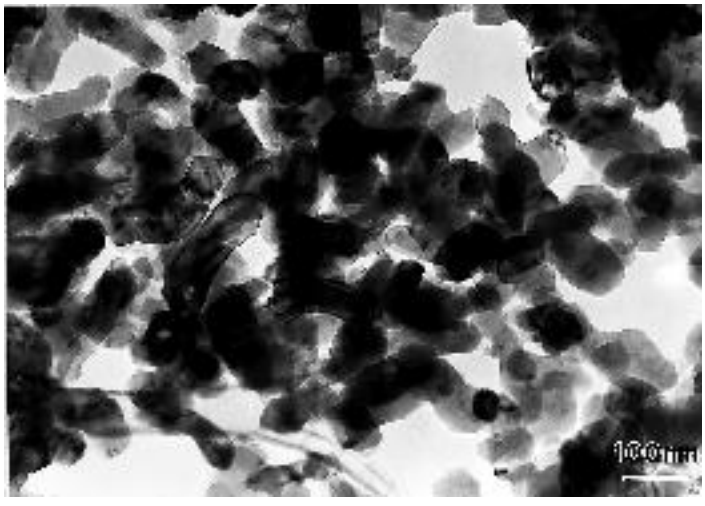

Figure 2. Bright-field transmission electron micrographs of MgO and Au/MgO catalysts, (a) undoped MgO, (b) 0.11 wt% Au, (c) 1.5 wt% Au, (d) 4.1 wt% Au, (e) 15 wt% Au. (Continued on next page.)

d

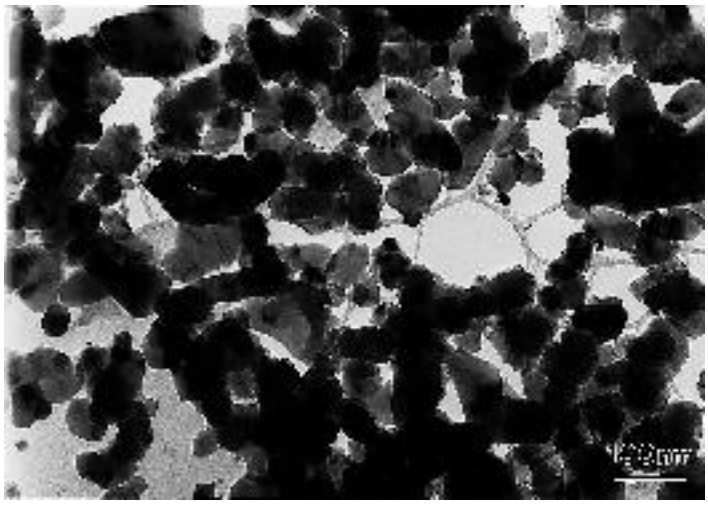

e

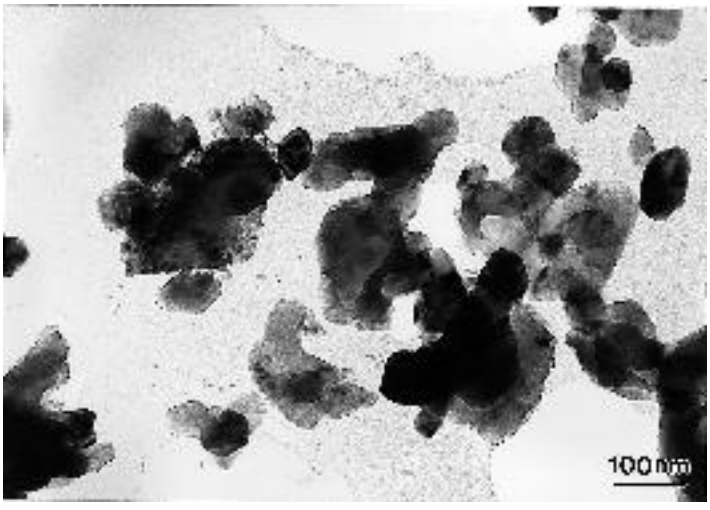

Figure 2. (Continued.)

could substitute for Mg^{2+} (0.72 Å) in the MgO lattice to produce additional anion or cation vacancies. The Au is initially added to the catalyst as $HAuCl_4$, but again Cl^- (1.81 Å) is considered to be too large to substitute for O^{2-} (1.38 Å) to produce cation defects. Hence, the mechanism by which this considerable grain growth effect occurs is still uncertain.

For all samples doped with Au, thin surface films are oberved by TEM. Experimental evidence that Au can grow in epitaxial thin film form on [001] MgO substrates has previously been presented by Tanaka et al. [15]. They demonstrated that the following epitaxial relationship frequently occurs between the Au film and the MgO support:

$$[100](001)\text{Au}//[100](001)\text{MgO}$$

The irregularity and magnitude of moiré fringe spacings found in our examples suggest that our crystalline rafts are not epitaxial with the support. For the parallel epitaxy situation quoted, the most prominent moiré fringe separations observed, assuming full relaxation has occurred, should be 6 and 8.5 nm. These correspond to the interference fringe periodicities expected between Au {100} and MgO {100} reflections respectively. The fact that the separations we observe are consistently smaller than this (i.e. 0.5–2 nm) suggests that the Au rafts are rotated considerably from the epitaxial orientation relation stated above. The moiré fringe contrast was observed in all the doped samples studied. The surface coverage of these features seemed rather similar irrespective of the Au loading. Furthermore, the average lateral extent of an individual thin film was also comparable throughout the series of samples. Since the surface area of the sample decreased considerably with increasing Au loading, this indicates that the total area of Au raft coverage per unit mass of catalyst decreases with increasing Au content. For the lowest Au doping level investigated (0.04 wt%) Mössbauer spectroscopy indicated the presence of an Au species that, in part, be assigned to the formation of these thin metallic rafts. The effect was not observed at higher Au doping levels, probably due to the decreased concentration of the Au

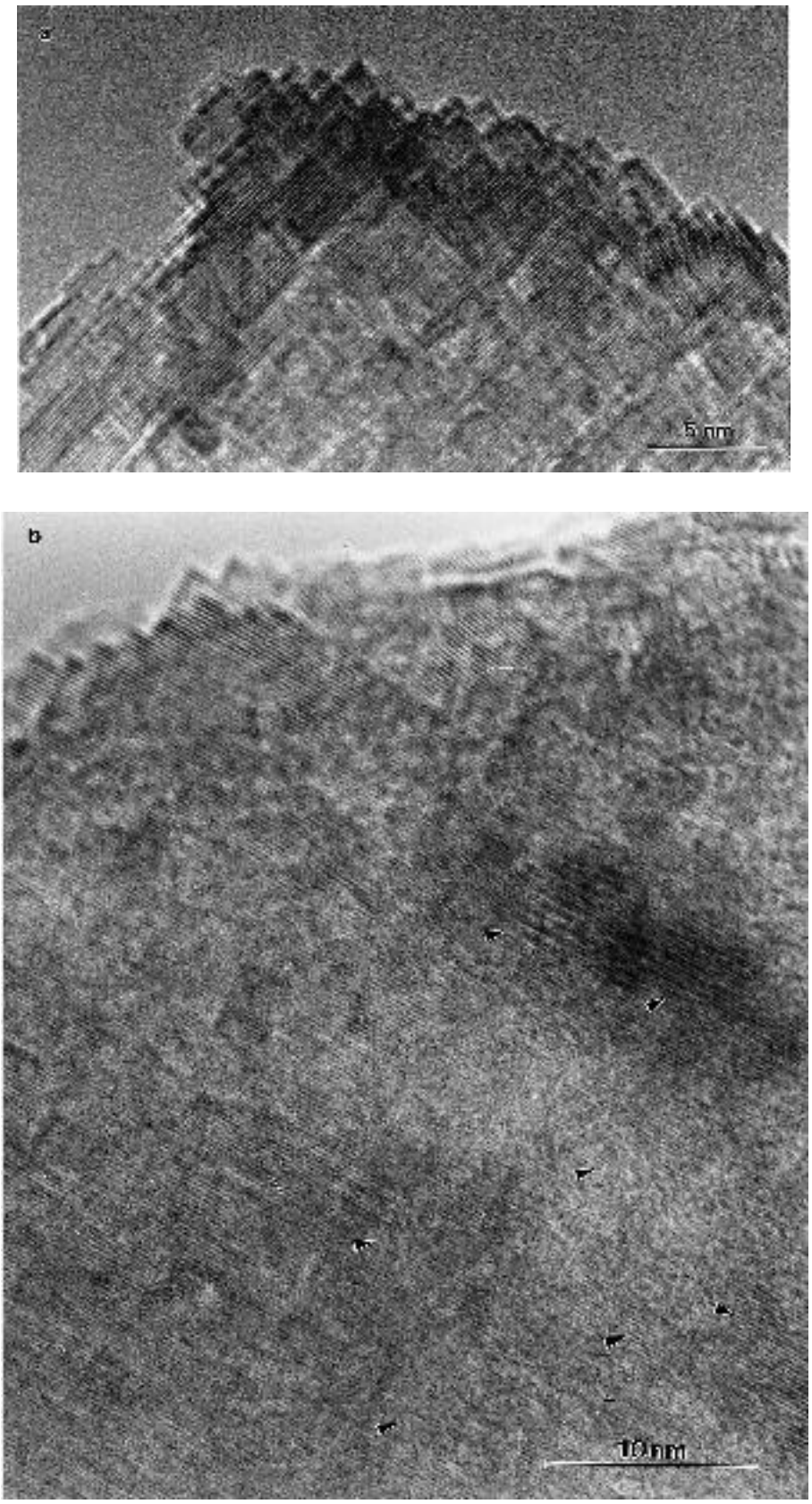

Figure 3. HREM images of (a) undoped MgO and (b) Au/MgO (in which patches of moiré fringe contrast are labelled in the latter).

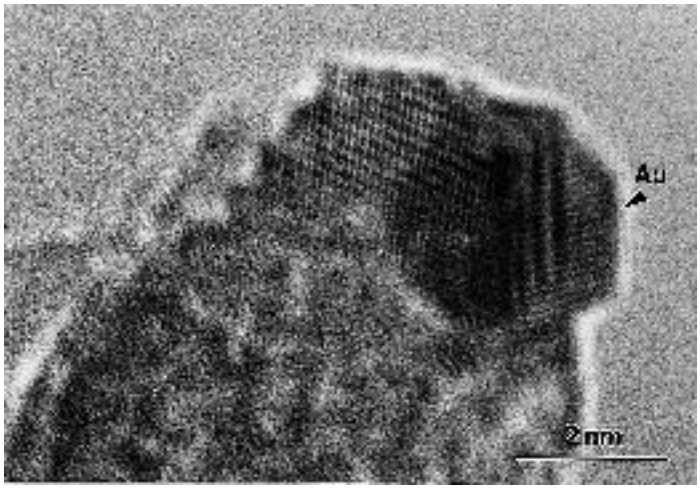

Figure 4. HREM image showing a discrete Au particle in a 3 wt% Au/MgO sample.

rafts relative to Au particles observed at Au loadings of $\geqslant$1.5 wt% Au.

It is therefore apparent that there are at least two distinct Au morphologies present in this series of catalysts, namely two-dimensional Au rafts and discrete three-dimensional Au particles (5–10 nm in diameter), and that the relative proportions of these morphologies varies as a function of the Au doping level. At the lowest doping levels only the thin Au films are visible, whereas at higher Au doping levels ($\geqslant$1.5%), Au particles are also observed. It should be noted at this point, however, that single Au atoms or smaller 2–3 atom clusters on the substrate could, in theory, also be present in some or all of the samples studied. Such a highly dispersed Au species is almost impossible to detect by HREM due to the intrinsic noise from the steps on the MgO support.

4.2. Relationship between catalyst structure and reactivity

The results for the catalytic conversion of methane over Au/MgO catalysts (table 1, figure 1) show that there is a significant effect with respect to Au concentration and three distinct types of activity are displayed by the Au/MgO catalysts used in this study. The first type is observed with very low Au loadings (e.g. 0.04 wt%) for which decreased intrinsic activity and methane coupling activity are observed. The second type is observed with intermediate concentrations of Au (up to ca. 2 wt% Au) for which the intrinsic activity increases with increasing Au concentration particularly for CO formation. The third mode of behaviour is observed with the higher Au concentrations ($\geqslant$5 wt% Au) for which the intrinsic activity increases with increasing Au concentration particularly for CO_2 formation. These variations in activity can be correlated with the structure of these catalysts.

In the absence of Au, MgO alone gives the products expected for the oxidative coupling of methane at this temperature (ethene, ethane, CO) together with the product of total combustion CO_2. However, the addition of a low concentration of Au (0.04 wt%) leads to a significant decrease in C_2 hydrocarbon formation as well as the intrinsic activity. In this case it appears that the Au blocks, or poisons, the surface sites associated with the formation of the methane coupling products since the yield of CO_2 is largely unaffected by the addition of 0.04% Au. Previous studies [11] with MgO prepared from the thermal decomposition of the hydroxide have shown that O^{2-} vacancies on the stepped surface planes are responsible for the the initial step in the oxidative coupling reaction, namely formation of methyl radicals from methane. It is therefore possible that these sites are sterically blocked at this Au concentration. Mössbauer spectroscopy of this sample indicates the presence of an Au species, at 15% of the total Au signal intensity, that can be assigned to the formation of a species closely associated with lattice O^{2-} of MgO, which is consistent with the blocking of such surface sites by Au. TEM studies show that at low concentration, Au is present primarily as thin two-dimensional surface patches. Possibly, these rafts, or even more disperse Au clusters, inhibit the sites responsible for methyl radical generation. This is an interesting observation since in the numerous previous studies of oxide and metal-doped oxide catalysts [8] few, if any, poisons for the methane coupling reaction have been identified.

As the Au loading increases, the intrinsic activity of the catalyst also increases as does the yield of CO. At higher Au concentrations ($>$ 2 wt% Au) the catalysts exhibit almost no selectivity to hydrocarbons and very high selectivity to CO_2 is observed, which is consistent with enhanced CO oxidation with these catalysts. Previous studies by Haruta et al. [4] have indicated that this reaction is catalysed by Au/MgO catalysts at ambient temperature. It would therefore be expected to be facile at the elevated temperature used in this study.

Haruta et al. [6] consider that the CO oxidation reaction is catalysed by discrete Au particles with diameters of ca. 5 nm, which are evident in the catalysts used in their studies containing 5 wt% Au and prepared by coprecipitation. The active site for such catalysts is considered [16] to be the interface between the Au particle and the oxide support. The Au/MgO catalysts in this study contain particles in the main with a 5–10 nm diameter and this is largely independent of the Au doping level at concentrations above 1.5%. However, in the our Au/MgO catalysts the MgO grain size also increases with the Au doping level. This together with the increasing concentration of Au particles leads to the formation of a larger interface area between the Au particles and MgO and it is these interface sites that are responsible for the oxidation of CO to CO_2.

In conclusion it is clear that Au/MgO catalysts show two distinct Au morphologies: (a) two-dimensional Au rafts and (b) discrete three-dimensional Au particles (5–10 nm in diameter). The two-dimensional Au rafts are observed as the main form of Au at low loadings and, interestingly, these are observed to poison the methane coupling activity of MgO. As the Au loading is increased the proportion of Au present as discrete particles increases and these are considered to be active for methane oxidation to CO and CO_2.

Acknowledgement

We thank BP for the provision of a studentship and EPSRC for financial support.

References

[1] B. Nkosi, N.J. Coville and G.J. Hutchings, J. Chem. Soc. Chem. Commun. (1988) 71.
[2] B. Nkosi, N.J. Coville, G.J. Hutchings, M.D. Adams, J. Friedl and F.E. Wagner, J. Catal. 128 (1991) 366.
[3] B. Nkosi, M.D. Adams, N.J. Coville and G.J. Hutchings, J. Catal. 128 (1991) 378.
[4] M Haruta, N. Yamada, T. Kobayashi and S. Iijima, J. Catal. 115 (1989) 301.
[5] D.A.H. Cunningham, T. Kobayashi, N. Kamijo and M. Haruta, Catal. Lett. 25 (1994) 257.
[6] M.L. Haruta, S. Tsubota, T. Kobayashi, H. Kageyama, M.J. Genet and B. Delmon, J. Catal. 144 (1993) 175.
[7] T. Hayashi, K. Tanaka and M. Haruta, Prp. Pet. Div., ACS Symp., New Orleans, 1996.
[8] G.J. Hutchings, M.S. Scurrell and J.R. Woodhouse, J. Chem. Soc. Chem. Commun. (1987) 1862.
[9] G.J. Hutchings, M.S. Scurrell and J.R. Woodhouse, J. Chem. Soc. Faraday Trans. I 85 (1989) 2507.
[10] J.S.J. Hargreaves, G.J. Hutchings and R.W. Joyner, Nature 348 (1990) 428.
[11] J.S.J. Hargreaves, G.J. Hutchings, R.W. Joyner and C.J. Kiely, J. Catal. 135 (1992) 576.
[12] E.E. Wolfe, ed., *Direct Methane Conversion by Oxidative Processes, Fundamental and Engineering Aspects* (Van Nostrand Reinhold, New York, 1992).
[13] P.M. Ajayan and L.D. Marks, Phys. Rev. Lett. 60 (1988) 585.
[14] P.M. Ajayan and L.D. Marks, Nature 338 (1989) 139.
[15] N. Tanaka, K. Kimoto and K. Mihama, Ultamicroscopy 39 (1991) 395.
[16] M. Haruta, A. Ueda, R.M. Torres Sanchez and K. Tanaka, Prp. Pet. Div., ACS Symp., New Orleans, 1996.